Advanced Composite Materials
Publication details, including instructions for authors and subscription information:
http://www.tandfonline.com/loi/tacm20

Tensile Properties of Carbon Fiber Composites with Different Resin Compositions at Cryogenic Temperatures

Myung-Gon Kim [a], Sang-Guk Kang [b], Chun-Gon Kim [c] & Cheol-Won Kong [d]

[a] Department of Aerospace Engineering, KAIST, 373-1 Kusong-dong, Yusong-gu, Daejeon 305-701, Korea

[b] Department of Aerospace Engineering, KAIST, 373-1 Kusong-dong, Yusong-gu, Daejeon 305-701, Korea

[c] Department of Aerospace Engineering, KAIST, 373-1 Kusong-dong, Yusong-gu, Daejeon 305-701, Korea;, Email: cgkim@kaist.ac.kr

[d] Department of Structures and Materials, Korea Aerospace Research Institute, 45, Eoeun-dong, Yuseong-gu, Daejeon 305-333, Republic of Korea

Version of record first published: 02 Apr 2012.

To cite this article: Myung-Gon Kim , Sang-Guk Kang , Chun-Gon Kim & Cheol-Won Kong (2010): Tensile Properties of Carbon Fiber Composites with Different Resin Compositions at Cryogenic Temperatures, Advanced Composite Materials, 19:1, 63-77

To link to this article: http://dx.doi.org/10.1163/156855109X434838

VSP

Advanced Composite Materials 19 (2010) 63–77

ADVANCED COMPOSITE MATERIALS
brill.nl/acm

Tensile Properties of Carbon Fiber Composites with Different Resin Compositions at Cryogenic Temperatures

Myung-Gon Kim [a], **Sang-Guk Kang** [a], **Chun-Gon Kim** [a,*] **and Cheol-Won Kong** [b]

[a] Department of Aerospace Engineering, KAIST, 373-1 Kusong-dong, Yusong-gu, Daejeon 305-701, Korea

[b] Department of Structures and Materials, Korea Aerospace Research Institute, 45, Eoeun-dong, Yuseong-gu, Daejeon 305-333, Republic of Korea

Received 15 January 2009; accepted 29 January 2009

Abstract

In this study, the tensile properties of carbon fiber reinforced polymer (CFRP) composites with different resin compositions were investigated in order to develop advanced composite materials for cryogenic use. Thermo-mechanical cyclic loading (up to 6 cycles) was applied to CFRP unidirectional laminate specimens from room temperature to −150°C. Tensile tests were then performed at −150°C using an environmental test chamber. In addition, matrix-dominant properties such as the transverse and in-plane shear characteristics of each composite model were measured at −150°C to examine the effects of resin formulation on their interfacial properties. The tensile tests showed that the composite models with large amounts of bisphenol-A epoxy and CTBN modified rubber in their resin composition had good mechanical performance at cryogenic temperatures (CTs).

Keywords

Carbon fiber reinforced composite, cryogenic, tensile property, resin composition

1. Introduction

Carbon fiber reinforced polymeric (CFRP) composites provide a promising material for the tank structure of launch vehicles that use liquid propellants because they are characterized by high specific strength and stiffness as well as by low thermal expansion. However, certain dramatic changes do take place in composite properties and their performances under cryogenic environments. In particular, under cryogenic conditions such as aging or cycling from room temperature (RT) to cryogenic temperature (CT), thermal stresses are induced by different coefficients of thermal expansion (CTEs) of the constituents at their interfaces. Consequently, cryogenic

* To whom correspondence should be addressed. E-mail: cgkim@kaist.ac.kr
Edited by KSCM

DOI:10.1163/156855109X434838

conditions cause microcracks that degrade the properties of composite materials by inducing damage such as potholing or delamination [1–3].

Recently, several studies have reported the effects of cryogenic conditions on composite properties and have suggested advanced materials for cryogenic use. Whitley and Gates [4] investigated the change of mechanical properties in CFRP laminate composites that had been aged at CT while being loaded. Results showed that a unidirectional laminate specimen that was aged with loads experienced 20% more degradation in tensile strength at CT than at RT. Some papers have investigated crack initiation by measuring acoustic emission sensors when composites are exposed to CT [5, 6]. Furthermore, Timmerman *et al*. [1] found that there is a large initial increase in the crack density, which generally reaches a constant value after a low level of cryogenic cycles. Kim *et al*. [7] also reported low thermo-mechanical cycle (up to 6 cycles) and temperature effects on the tensile properties of a CFRP composite. In this paper, it was found that tensile strength increased more at CT after a few of cycles than when a specimen did not undergo any cycles.

Previous works have also examined advanced composite materials for cryogenic use. Sawa *et al*. [8] showed the improved fracture toughness of epoxy resins at CT by using the molecular formulation of several epoxies. For the cracking resistance under cryogenic environments, some studies have examined the microcrack density and its propagation after cryogenic cycles in CFRP composites that had different fibers and resin compositions [1, 3]. Also, it has been proven that microcracks can be reduced by incorporating nano/mico-sized fillers such as Al_2O_3 or silica particles and clay in the resin formulation [9–11].

In this study, six types of carbon fiber reinforced composites were developed for cryogenic use by formulating different resins and additives, and the tensile properties of the material systems were measured after low thermo-mechanical cycles at CT. As a result, we found a suitable resin composition of a carbon fiber reinforced composite for high cryogenic mechanical performances.

2. Material Systems

Table 1 shows the resin composition of the graphite fiber reinforced composites that have been developed in this study for cryogenic use. The resins of each composite model were formulated using a mixture of commercial epoxy resins. Aliphatic polyamine dicyandiamide (DICY) was used as a hardening agent and diuron (DCMU) was used as an accelerator for curing. Also, a graphite fiber, T700 from Toray Industries Inc., was used for reinforcement in each composite model.

In Table 1, CU125NS is a graphite/epoxy prepreg model manufactured by Han-Kuk Fiber Glass Corporation. The other six kinds of models were reinforced with the same graphite fibers as in CU125NS but were formulated with different types and blend ratios of epoxy resins and additives that were used as toughening agents. The resins of each composite model were formulated using a mixture of phenolic

Table 1.
Resin formulation of graphite/epoxy composite models

Model	Epoxy type		Filler (phr)
CU125NS	Phenolic novolac	Bisphenol-A (solid, liquid)	Thermoplastic (1.5)
Type A	Phenolic novolac	Bisphenol-A (solid, liquid)	Thermoplastic (4.5)
Type B	Phenolic novolac	Bisphenol-A (solid, liquid)	Liquefied CTBN rubber (4.5)
Type C	Phenolic novolac	Bisphenol-A (solid, liquid)	–
Type D	Phenolic novolac	Bisphenol-A (solid)	Liquefied CTBN rubber (4.5)
Type E	Phenolic novolac	Bisphenol-A (solid, liquid)	Solidified CTBN rubber (3.0)
Type F	Phenolic novolac	Bisphenol-A (solid, liquid)	Liquefied CTBN rubber (5.0)
Remarks	Different blend ratio for each model		

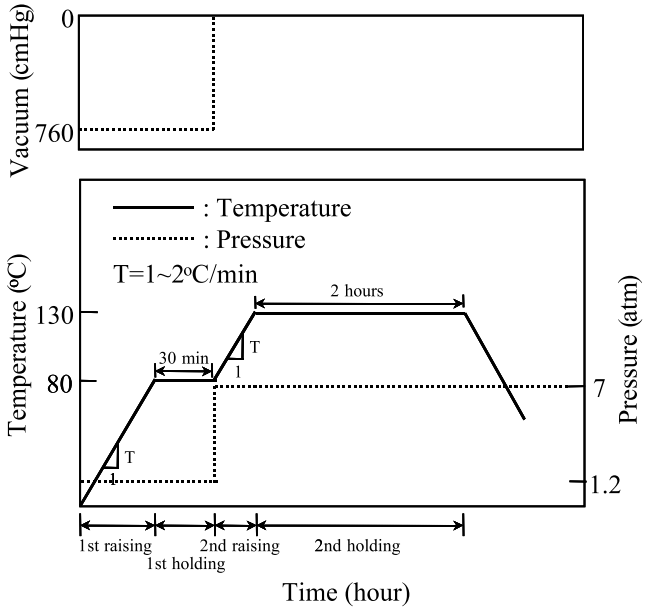

Figure 1. Curing cycle for graphite/epoxy laminates in an autoclave.

novolac epoxy and bisphenol-A epoxy. Type A and Type D contain more phenolic novolac epoxy than bisphenol-A in their resin composition, while Type B, Type C, Type E and Type F have more bisphenol-A. Also, thermoplastic and carboxyl terminated butadiene acrylonitrile (CTBN) modified rubber with differing parts per hundred resin (phr) were incorporated into the resin mixture as additives.

The laminates of each composite model were fabricated by means of autoclave curing. Figure 1 presents the history of pressure, temperature, and vacuum conditions as a function of time during the cure.

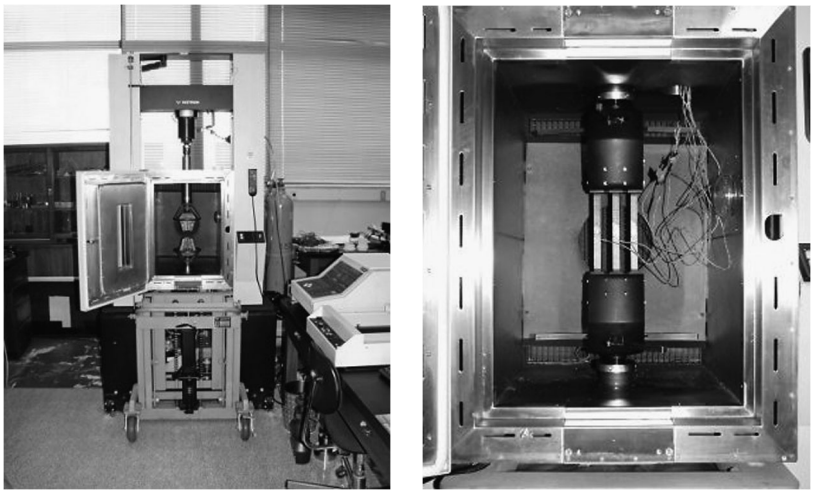

(a) (b)

Figure 2. (a) Experimental setup; (b) 3-jaw tensile grip.

3. Experimental

3.1. An Environmental Test Chamber and Strain Measuring Method

In this study, an environmental test chamber was used to set up the cryogenic tensile test. The environmental chamber, Instron 3119-407, can cool the temperature down to −150°C by evaporating the liquid cryogenic medium.

As shown in Fig. 2(a), the grips and loading bars of the apparatus were inserted into the environmental chamber and the gaps between them were sealed and insulated with asbestos. The time needed to cool down to below room temperature generally depends on the pressure level of the vessel containing the liquid medium, so a pressurizing device was used to maintain the evaporating pressure of 1.5 atm (22 psi) and, consequently, to keep the cooling time constant. Liquid nitrogen (LN_2) was used as a cryogenic medium. The wedge-typed 3-jaw tensile grip, which reduces the time and cost involved in the thermo-mechanical cycle as it can apply equal loads to 3 specimens simultaneously, was used during the thermo-mechanical cycles but a single-jaw tensile grip was used during the tensile tests.

Electric strain gages and lead wires for cryogenic use were adopted to accurately measure the strain data at the cryogenic temperature. In addition, the apparent strain induced by the gages themselves increases when temperature changes from RT to CT. Therefore, a Wheatstone half bridge circuit was adopted to compensate for the thermal strains induced by the gages.

3.2. Specimen Preparation

Graphite/epoxy laminates with different resin compositions were prepared for measuring tensile and shear properties. The specimen configurations and test procedures were in accordance with ASTM D 3039. Laminates with stacking sequences $[0_8]_T$

and $[90_{16}]_T$ were stacked to obtain the longitudinal and transverse tensile properties of each composite model, respectively. To obtain the in-plane shear properties of the composite models, a $[\pm 45]_{4S}$ configuration of the prepregs was stacked and fabricated according to ASTM D 3518. Also, during the tensile tests at $-150°C$, the specimen tabs that were made of a glass/epoxy woven fabric composite, which is commonly used as a tab material, cause separation to occur between the tab and the laminate when a high load is applied to the specimen at CT. This occurs because shear stress is induced due to the different CTEs between the tab material and the laminate specimen. Consequently, an emery cloth with a relatively low stiffness was used as a tab material because it can follow the thermal contraction of the laminate specimen.

3.3. Thermo-Mechanical Cycle

To simulate the propellant tank of a launch vehicle that undergoes thermal and mechanical loads simultaneously, 3-jaw tensile grips were used to apply thermo-mechanical cycles to three specimens at the same time. The thermo-mechanical cycles were only applied to the laminate specimen of $[0_8]_T$ to investigate the effects of low cycles on the longitudinal tensile properties of each composite model.

The thermo-mechanical cycling process, from RT to $-150°C$, is shown in Fig. 3. The cycling load was applied to the specimens by half of the failure load at RT, which was determined by safety factors considered in the design of the tank structure. A pressurizing device was used to keep the same cooling time from RT to the target temperatures for each specimen. While the temperature was cooled to the target temperature, induced thermal loads in the specimen were removed up to the thermal equilibrium of the specimen to evaluate its pure mechanical tensile properties at the target temperatures. It took about 30 min to reach the thermal equilibrium

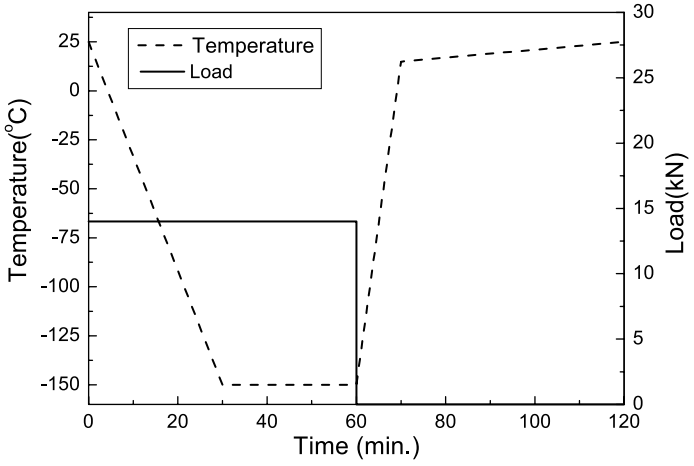

Figure 3. Thermo-mechanical cycle for unidirectional laminate specimens.

state and about 2 h to complete 1 cycle. After each cycle, the moisture that formed in the specimen was eliminated using a drying device at RT.

3.4. Tensile Tests

3.4.1. Tensile Tests for Longitudinal Tensile Property

This study examined the effect of a thermo-mechanical cycle on the tensile properties of graphite/epoxy composite models. The tensile stiffness and strength of each laminate specimen were measured after 6 thermo-mechanical cycles, as shown in Fig. 3 [7]. During tensile tests, however, interference induced by congealed grease or by vapor between grip-faces and grip-heads caused the specimen to slide from the grips. Therefore, to prevent this phenomenon when specimens were tested at CT, a preload of as much as 5 kN was applied before the tests were initiated.

3.4.2. Tensile Tests for Transverse and In-plane Shear Properties

For each composite model, laminates with stacking sequences of $[90_{16}]_T$ and $[\pm 45]_{4S}$ were used to measure the longitudinal tensile properties and in-plane shear properties, respectively. These properties can indirectly show the changes not only in the matrix dominant properties but also in the interfacial properties between the fiber and matrix as the resin constituent is altered [12].

A tensile test for measuring transverse properties was performed both at RT and at −150°C. The thermal load induced during cooling and the thermal equilibrium was steadily removed at a rate of 0.1 mm/min. After the specimen reached thermal equilibrium, the tensile stiffness and strength were measured through tensile tests at a rate of 0.2 mm/min. An identical transverse tensile test was also performed for the in-plane shear test at a rate of 2.0 mm/min.

4. Results and Discussion

4.1. Longitudinal Tensile Properties

Longitudinal tensile properties were investigated at −150°C after the 6 thermo-mechanical cycles had been performed. To examine the thermal effect on the specimens, six mechanical cycles were applied to each composite model at RT. Figure 4 shows the results of longitudinal stiffness (a) and strength (b) for the specimens that experienced non-cycling, 6-cycling at RT, and 6-cycling from RT to −150°C.

It is essential that the specimens have the same fiber volume fraction in order to accurately compare the stiffness and strength of each composite model. Therefore, referring to ASTM D 2584, we obtained the fiber volume fraction for each laminate which was identical to that used in the tensile test. The average fiber volume fractions of each laminate are presented in Table 2. As shown in Table 2, however, each composite laminate has a different fiber volume fraction. Consequently, additional work is needed so that the tensile stiffness and strength can be compared at the same fiber volume fraction for each model.

In this study, the tensile stiffness and strength of each composite model were compared at the same fiber volume fraction using test results and the equations of

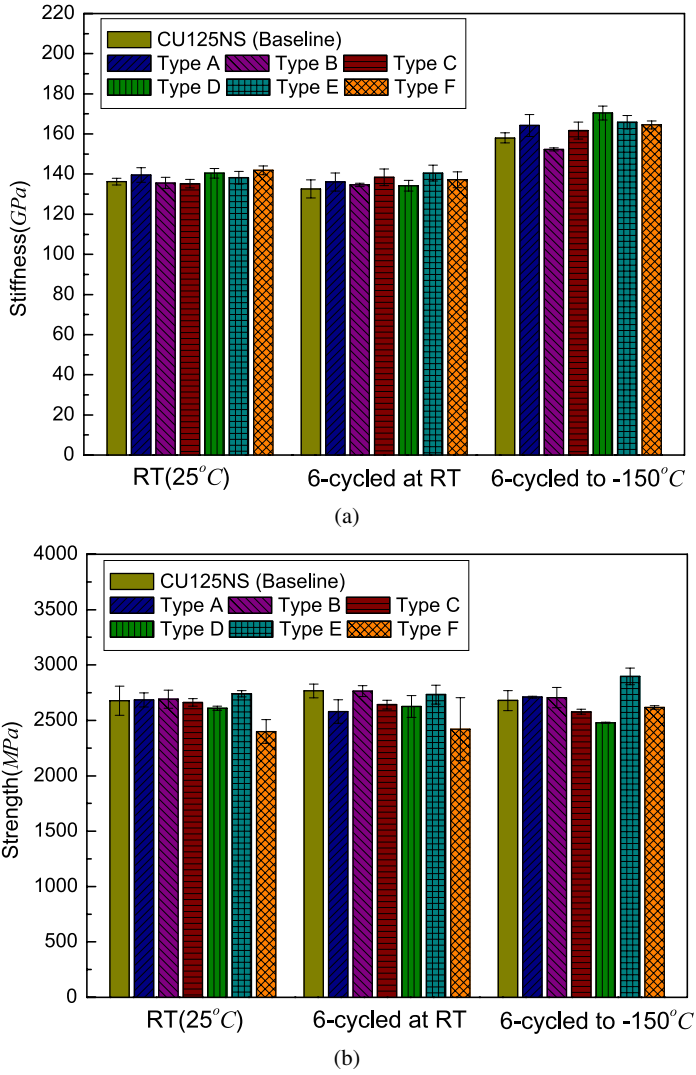

Figure 4. The longitudinal stiffness (a) and strength (b) of graphite/epoxy UD laminate models. This figure is published in color on http://www.ingentaconnect.com/content/vsp/acm

Table 2.
Fiber volume fraction of each composite model

Model	CU125NS	Type A	Type B	Type C	Type D	Type E	Type F
V_f	0.70	0.72	0.66	0.69	0.75	0.72	0.69

rule of mixture. Equations (1) and (2) show the equations of rule of mixture for estimating the stiffness and strength of a composite, respectively. In (1) and (2),

E_{f1} and E_{f2} are the tensile stiffness of the fiber along the fiber direction and toward the transverse direction, respectively, and the relation between these two factors can be estimated by $E_{f1} \approx 15E_{f2}$, according to the manufacturer's data sheet [13].

Additionally, in equation (2), s_m and s_{mf1} mean the ultimate strength of the matrix and the stress applied in the matrix at fiber breakage, respectively. It is assumed that $s_m = s_{mf1}$ on the grounds that the strength of the matrix has little influence on the longitudinal strength of the composite. The transverse strength of the composite was calculated using strain concentration factor, F, assuming that the fibers in the laminate specimen have a square array [14].

$$E_1 = E_{f1}v_f + E_m(1 - v_f), \qquad \frac{1}{E_2} = \frac{v_f}{E_{f2}} + \frac{(1 - v_f)}{E_m}, \tag{1}$$

$$s_L = s_{f1}v_f + s_{mf1}(1 - v_f), \qquad s_T = \frac{E_2 s_m}{E_m F}, \quad \text{where } F = \frac{1}{\frac{d}{s}[\frac{E_m}{E_{f2}} - 1] + 1}. \tag{2}$$

The effective stiffness and strength of the fiber and matrix were calculated using equations (1), (2) and longitudinal and transverse stiffness and strength of each laminate specimen, such as E_1, S_L to the fiber direction and E_2, S_T transverse to the fiber direction with fiber volume fraction (v_f). Consequently, for all composite models, the longitudinal stiffness and strength were investigated at a fiber volume fraction of 0.7, which was exactly the same as that in the baseline model, CU125NS. The results are presented in Fig. 5.

After six mechanical cycles at RT, all composite models show a higher tensile stiffness than that shown by CU125NS, with the exception of Type D, as shown in Fig. 5(a). Of all the models, Type B shows the highest stiffness at RT after RT-cycling and Type F shows the highest at −150°C after CT-cycling, which is about 6.2% higher than that shown by CU125NS. Overall, each composite model after CT-cycling shows higher stiffness than that after RT-cycling and there is little difference among them after CT-cycling. Therefore, it is assumed that, when the composites are fabricated using the same reinforcing fibers, variations in resin composition have little influence on the stiffness of the composite models at CT after low thermo-mechanical cycles.

On the other hand, Fig. 5(b) shows that tensile strength varies widely with changes in resin composition. In particular, Type B showed the highest strength both at RT and at −150°C after the thermo-mechanical cycles were completed; these measurements were about 6% and 7% higher, respectively, than those recorded for CU125NS at the same temperatures. Although Type E also showed strength about 5% higher than CU125NS at −150°C, the strength of the other composite models was actually less than that of CU125NS after RT-cycling and CT-cycling. Type A, Type C, and Type F showed almost the same strength, but Type D showed about 14% less strength than CU125NS. From these results, it is speculated that having

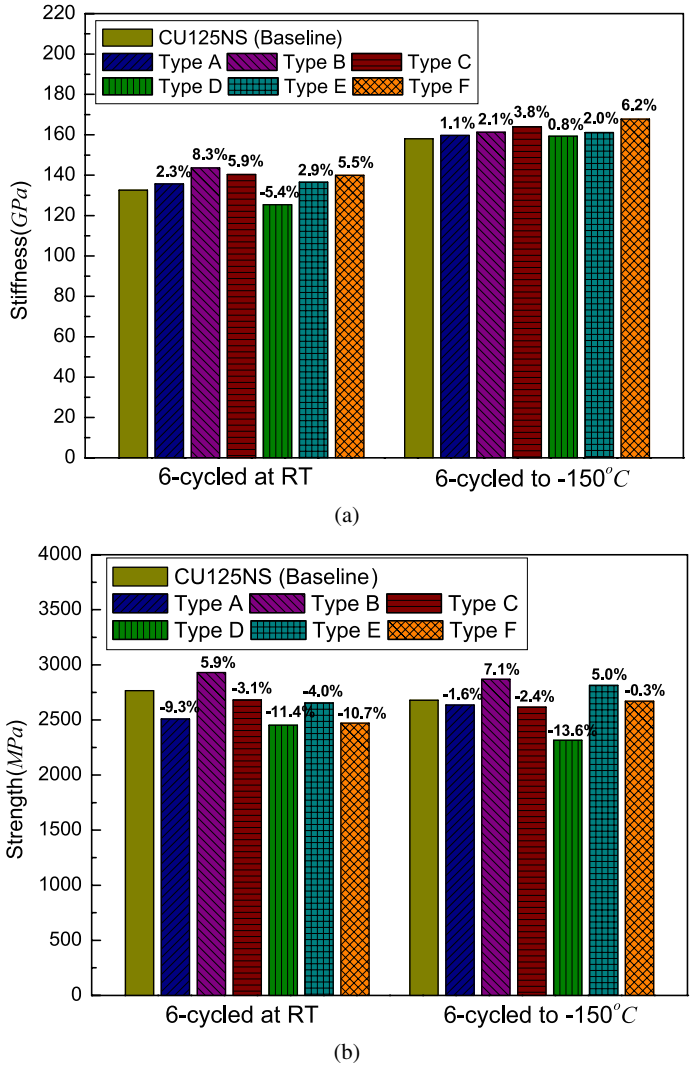

Figure 5. The longitudinal stiffness (a) and strength (b) of graphite/epoxy UD laminate models when the fiber volume fraction is modified to 0.7. This figure is published in color on http://www.ingentaconnect.com/content/vsp/acm

more bisphenol-A epoxy than phenolic novolac in the formulation of the composite results in good tensile performance at −150°C. This speculation is especially compelling since the composite models that contained CTBN modified-rubber filler showed the highest tensile strength of those tested. It is considered, then, that resin compositions with more bisphenol-A epoxy and CTBN modified rubber experience greater interfacial shear strength between the fiber and the matrix and, therefore, they are also affected less by microcracking. Consequently, the strength of composites can differ even when the same fiber is used in each.

4.2. Transverse Tensile Properties

Figure 6 shows the tensile transverse stiffness and strength of each composite model at RT and at −150°C. As Fig. 6(a) shows, the tensile stiffness of each composite model has lower overall values than CU125NS. However, there is not a great deal of variation in the tensile stiffness of the models. At −150°C, with little difference between them, Type A and Type D showed higher tensile stiffness than CU125NS. In addition, Type C showed a relatively low stiffness at −150°C, which is considered to be the result of not having additives in its resin composition. Therefore, it

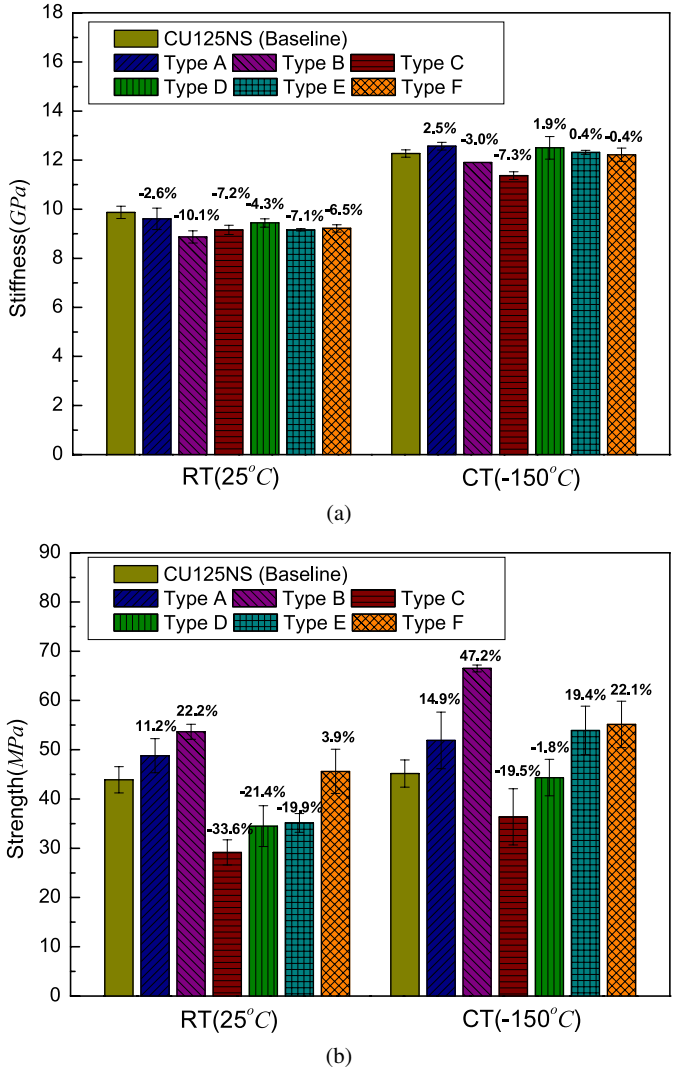

Figure 6. The transverse stiffness (a) and strength (b) of graphite/epoxy laminate models. This figure is published in color on http://www.ingentaconnect.com/content/vsp/acm

is speculated that additives like fillers influence the improvement of the transverse tensile stiffness of the composite at CT.

In the results of Fig. 6(b), the transverse tensile strength of the composite models is vastly different according to changes in the resin formulation, unlike for transverse stiffness. Above all, it is obvious that strength values behave similarly at RT and at −150°C for each composite model. In addition, Type B showed the highest strength both at RT and at −150°C, which was 47% higher than that shown by CU125NS. Also, Type E and Type F both showed the increases by 20% and 15% more than CU125NS at −150°C. Type C, however, decreased by 20% compared to CU125NS at −150°C.

Test results indicate, therefore, that changing the resin formulation affects the transverse tensile stiffness of each composite model more than the transverse tensile strength, and the trends pertaining to transverse strength are similar to those for longitudinal tensile strength. In other words, the two tests proved that, of all the models tested, Type B and Type E had the highest strength at −150°C. Also, it is well known that interfacial bonding properties can be represented by the transverse strength of unidirectional laminates [15]. Consequently, it is possible that having a large portion of bisphenol-A epoxy in the resin composition as well as the addition of CTBN modified-rubber affects the increase in tensile strength at CT.

4.3. In-plane Shear Properties

To investigate the interfacial properties of composite models, an in-plane shear test was performed using $[\pm 45]_{4S}$ laminate specimens, under the consideration that the interfacial shear strength had affected the change of strength of the composite models. Also, this in-plane shear test with $[\pm 45]_{4S}$ can be indirectly used to compare interfacial properties and quantitative properties. Figure 7 shows the in-plane shear stiffness and strength of each composite model at RT and at −150°C.

In Fig. 7(a), composite models such as CU125NS and Type A and Type D, which have a large portion of phenolic novolac in their resin composition as well as thermoplastic fillers, showed higher shear stiffness at both RT and −150°C than Type B, Type E, and Type F, which contained more bisphenol-A and CTBN modified rubber fillers than the other models, except Type C. However, the differences were not great and the shear stiffness of all composite models has a trend to increase as temperature decreases.

As with stiffness, the shear strength of all composite models increased at CT, as shown in Fig. 7(b). Additionally, it is found that the results of shear strength testing are similar to those of transverse strength testing at −150°C. Consequently, by comparing the above test results for each composite model, it is speculated that Type B, Type E, and Type F, which are all formulated with a large portion of bisphenol-A epoxy and CTBN modified rubber in their resin composition, have better interfacial properties at CT.

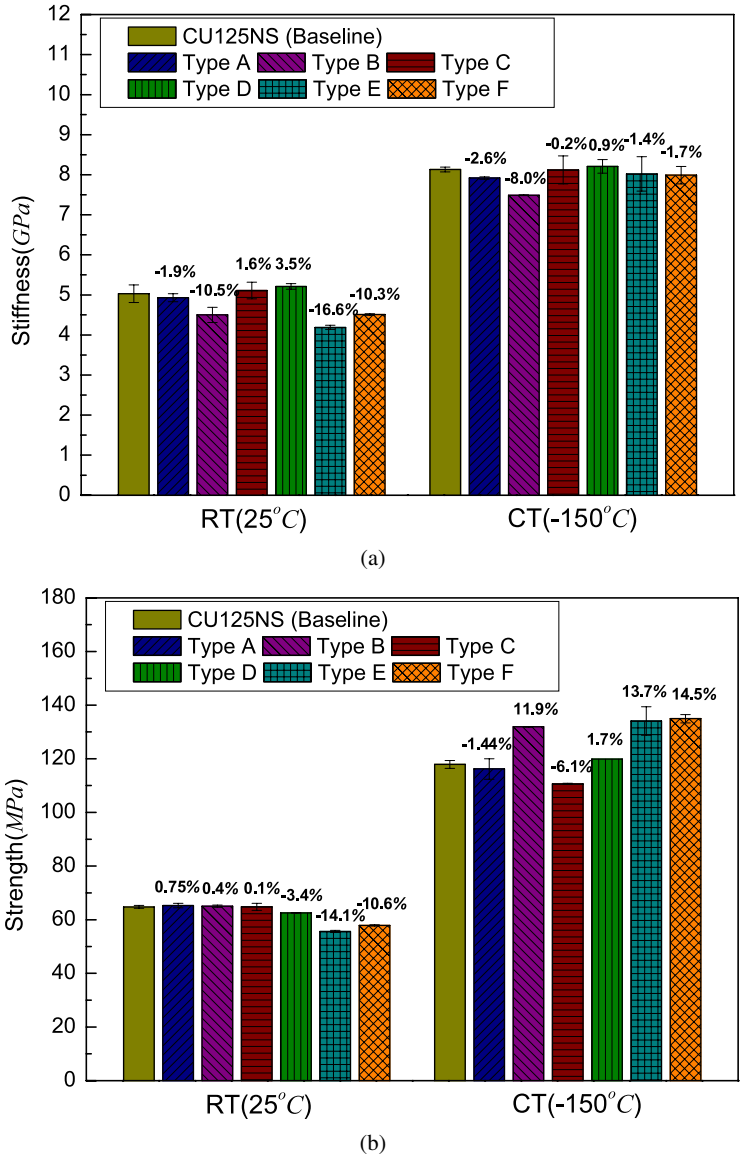

Figure 7. The in-plane shear stiffness (a) and strength (b) of graphite/epoxy laminate models. This figure is published in color on http://www.ingentaconnect.com/content/vsp/acm

4.4. Cryogenic Aging Effects

In this study, thermo-mechanical loading cycles that were exposed to a low temperature over a long period of time were applied to composite models to investigate the effect of cryogenic aging on mechanical properties. The procedure of cryogenic aging was performed by keeping the equilibrium time in Fig. 3 to 9 h at −150°C. Type B and Type F were adopted because they showed the highest strength and

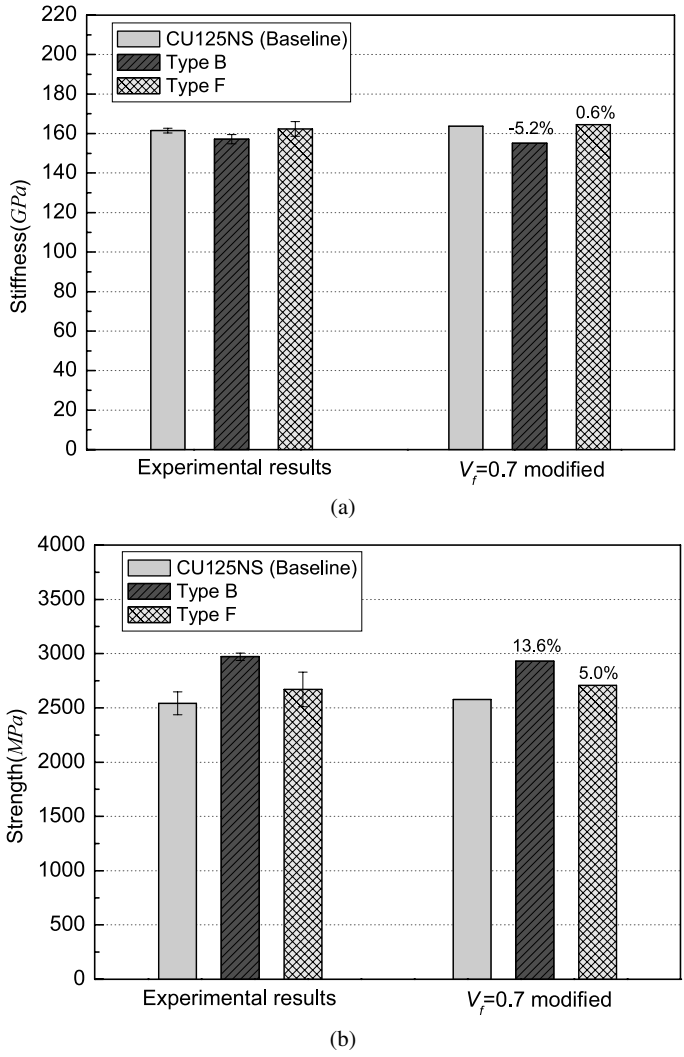

Figure 8. The longitudinal stiffness (a) and strength (b) of laminate models after long-term exposure at −150°C.

stiffness at CT of all the composite models, and CU125NS was used as the baseline model. Up to six aging cycles were performed.

The properties of the models were evaluated through the same procedure as that given in Section 4.1. Figure 8 shows the longitudinal tensile stiffness and strength of each adopted model. As shown in Fig. 8(a), Type F and CU125NS show higher stiffness than Type B after the aging cycles. All of the composite models, however, showed higher stiffness at CT than at RT. Overall, Type B shows the highest tensile strength after the aging cycles, which is about 13.6% higher than CU125NS. Also, it was found that the aging for 9 h at −150°C has little influence in the longitudinal properties.

5. Conclusion

In this study, for the purpose of developing carbon fiber reinforced composites for cryogenic use, the mechanical properties of the composite models that had been developed through formulating resin constituents were measured both at RT and at −150°C after thermo-mechanical cycles had been performed.

As a result of testing the tensile strength of seven types of graphite/epoxy composite models, it was found that the longitudinal tensile stiffness was influenced only a little as the resin formulation changed and as additives were added to their resin composition after the six thermo-mechanical cycles from RT to −150°C. Longitudinal tensile strength, however, was greatly influenced by resin composition. Especially, composite models that were formulated with a large portion of bisphenol-A epoxy and CTBN modified rubber in their resin composition showed high strength at CT. To analyze the test results, transverse and in-plane shear properties were measured at CT. Quantitative comparisons of test results show that the interfacial properties that were altered by the different resin compositions affected the longitudinal tensile strength of each composite model.

In addition, thermo-mechanical cycles that experienced long-term exposure to low temperatures were applied to composite models to investigate the effect of cryogenic aging on the mechanical properties of the composites. The test results showed that there was hardly any difference in the longitudinal properties between after only cycles and after aging cycles.

Acknowledgements

This research was carried out with Han-Kuk Fiber Glass Co. Ltd. The authors would like to thank the Korea Aerospace Research Institute, Korea, for the financial support.

References

1. J. F. Timmerman, M. S. Tillman, B. S. Hayes and J. C. Seferis, Matrix and fiber influences on the cryogenic microcracking of carbon fiber/epoxy composites, *Composites Part A* **33**, 323–329 (2002).
2. V. T. Bechel, M. B. Fredin, S. L. Donaldson and R. Y. Kim, Effect of stacking sequence on microcracking in a cryogenically cycled carbon/bismaleimide composite, *Composites Part A* **34**, 663–672 (2003).
3. V. T. Bechel, J. D. Camping and R. Y. Kim, Cryogenic/elevated temperature cycling induced leakage paths in PMCs, *Composites Part B* **36**, 171–182 (2005).
4. K. S. Whitley and T. S. Gates, Thermal/mechanical response and damage growth in polymeric composites at cryogenic temperatures, *AIAA* **1416** (2002).
5. T. Aoki, T. Ishkawa, H. Kumazawa and Y. Morino, Cryogenic mechanical properties of CF/polymer composites for tanks of reusable rockets, *AIAA* **1605** (2000).
6. R. Y. Kim and S. L. Donaldson, Development of damage in composites under thermomechanical loading, in: *Proc. of ICCM14* (2003).

7. M. G. Kim, S. G. Kang, C. G. Kim and C. W. Kong, Tensile response of graphite/epoxy composites at low temperatures, *Compos. Struct*. **79**, 52–57 (2007).
8. F. Sawa, S. Nishijima and T. Okada, Molecular design of an epoxy for cryogenic temperatures, *Cryogenics* **35**, 767–769 (1995).
9. M. Hussain, A. Nakahira, S. Nishijima and K. Niihara, Evaluation of mechanical behavior of CFRC transverse to the fiber direction at room and cryogenic temperature, *Composites Part A* **31**, 173–179 (2000).
10. J. Lee, R. Patton, J. Schneider, C. Pittman, J. Ragsdale, L. Wang and T. DeLay, Performance of modified epoxies in composites at cryogenic temperatures, in: *SAMPE Inter. Sympos. and Exhibition*, Long Beach, CA, USA (2004).
11. J. F. Timmerman, B. S. Hayes and J. C. Seferis, Nanoclay reinforcement effects on the cryogenic microcracking of carbon fiber/epoxy composites, *Compos. Sci. Technol.* **62**, 1249–1258 (2002).
12. J. K. Kim and Y. Mai, *Engineered Interface in Fiber Reinforced Composites*, 1st edn, Vol. 3, pp. 61–74. Elsevier, The Netherlands (1998).
13. C. C. Chamis, Simplified composite micromechanics equations for mechanical, thermal and moisture-related properties, *Engineers' Guide to Composite Materials*. ASM International, Materials Park, OH, USA (1987).
14. J. A. Kies, Maximum strains in the resin of fiber glass composites, *U.S. Naval Research Laboratory Report* **5752** (1962).
15. M. S. Madhukar and L. T. Drzal, Fiber-matrix adhesion and its effects on composite mechanical properties: II. Longitudinal (0°) and transverse (90°) tensile and flexural behaviour of graphite/epoxy composites, *J. Compos. Mater.* **25**, 958–991 (1991).